



## Growth studies and optical properties of $\text{Zn}_{1-x}\text{Cd}_x\text{O}$ films grown by metal-organic chemical-vapor deposition

Corinne Sartel, Nadia Haneche, Christèle Vilar, Gaelle Amiri, Jean-Michel Laroche, François Jomard, Alain Lusson, Pierre Galtier, Vincent Sallet, Christophe Couteau, et al.

### ► To cite this version:

Corinne Sartel, Nadia Haneche, Christèle Vilar, Gaelle Amiri, Jean-Michel Laroche, et al.. Growth studies and optical properties of  $\text{Zn}_{1-x}\text{Cd}_x\text{O}$  films grown by metal-organic chemical-vapor deposition. Journal of Vacuum Science & Technology A, 2011, 29 (3), pp.03A114. 10.1116/1.3567960 . hal-02269663

**HAL Id: hal-02269663**

**<https://utt.hal.science/hal-02269663>**

Submitted on 7 Dec 2021

**HAL** is a multi-disciplinary open access archive for the deposit and dissemination of scientific research documents, whether they are published or not. The documents may come from teaching and research institutions in France or abroad, or from public or private research centers.

L'archive ouverte pluridisciplinaire **HAL**, est destinée au dépôt et à la diffusion de documents scientifiques de niveau recherche, publiés ou non, émanant des établissements d'enseignement et de recherche français ou étrangers, des laboratoires publics ou privés.

# Growth studies and optical properties of $\text{Zn}_{1-x}\text{Cd}_x\text{O}$ films grown by metal-organic chemical-vapor deposition

Corinne Sartet,<sup>a)</sup> Nadia Haneche, Christèle Vilar, Gaelle Amiri, Jean-Michel Laroche, François Jomard, Alain Lusson, Pierre Galtier, and Vincent Sallet<sup>b)</sup>  
*Groupe d'Etude de la Matière Condensée (GEMaC), CNRS–Université de Versailles St.-Quentin, 1 Place A. Briand, 92195 Meudon Cedex, France*

Christophe Couteau, Jenny Lin, Roy Aad, and Gilles Lérondel  
*Laboratoire de Nanotechnologie et d'Instrumentation Optique, Institut Charles Delaunay and UMR6279 STMR, CNRS–Université de Technologie de Troyes, 12 rue Marie Curie, BP 2060, Troyes Cedex, France*

(Received 10 September 2010; accepted 28 February 2011; published 18 March 2011)

Heteroepitaxial growths of  $\text{Zn}_{1-x}\text{Cd}_x\text{O}$  films were performed on *R*-oriented sapphire substrates by metal-organic chemical-vapor deposition. The authors carried out secondary ion mass spectrometry analysis, scanning electron microscopy, photoluminescence, and ellipsometric measurements to investigate the incorporation of cadmium in the layers, as well as its influence on the optical properties. Compositions up to 5.5% Cd were obtained, tuning the photoluminescence emission from 3.36 (ZnO) to 3.1 eV and increasing the refractive index at 600 nm from 1.94 to 2. © 2011 American Vacuum Society. [DOI: 10.1116/1.3567960]

## I. INTRODUCTION

ZnO is now considered as one of the most promising materials for optoelectronic applications in the blue and uv regions. To tune its wide band gap (3.37 eV), researchers have studied several approaches of alloying the binary ZnO with  $\text{MgO}$ ,<sup>1,2</sup>  $\text{BeO}$ ,<sup>3</sup> and  $\text{CdO}$ .<sup>4–6</sup> A great effort of research has been devoted to  $\text{Zn}_{1-x}\text{Mg}_x\text{O}$  solid solutions, which has led to the creation of original ZnO/ZnMgO quantum wells<sup>7</sup> and high mobility two-dimensional (2D) electron gas.<sup>8</sup> Due to the high toxicity of metallic beryllium and beryllium oxide, only a few papers have been published on  $\text{Zn}_{1-x}\text{Be}_x\text{O}$  ternary compound. Alloying ZnO with CdO is an approach that allows for the decrease of ZnO band gap despite the fact that ZnO and CdO crystallize in different symmetries, i.e., respectively, wurzite and cubic. Also, the solubility limit of cadmium in the ZnO matrix under equilibrium conditions is only 2%, so that one may expect some difficulties in achieving single phase  $\text{Zn}_{1-x}\text{Cd}_x\text{O}$  films containing high Cd contents. Until now, various techniques have been employed to grow ZnCdO alloys under nonequilibrium conditions. Among these techniques are molecular beam epitaxy,<sup>9</sup> pulsed laser deposition,<sup>4</sup> metal-organic chemical-vapor deposition (MOCVD),<sup>6,10,11</sup> magnetron sputtering,<sup>12</sup> and (CdO+ZnO) powder sintering.<sup>13</sup> A reduction in the band gap of 1.55 eV was reported for alloys at 69% Cd concentration.<sup>14</sup>

To characterize the optical properties of  $\text{Zn}_{1-x}\text{Cd}_x\text{O}$  films, photoluminescence (PL) studies have been carried out. In particular, Lusson *et al.*<sup>15</sup> reported on localization effects, i.e., excitons trapped in potential fluctuations due to alloy at the atomic scale. Besides active properties, like photoluminescence, band gap tuning is also important for the control of

passive optical properties such as the index of refraction. Recently, Mares *et al.*<sup>16</sup> showed, by means of transmission and ellipsometric measurements, that a refractive index shift of typically 0.25 in the visible range can be obtained using  $\text{Zn}_{1-x}\text{Cd}_x\text{O}$  with *x* varying from 2% to 73%.

In this work,  $\text{Zn}_{1-x}\text{Cd}_x\text{O}$  layers have been deposited on *R*-sapphire substrates by MOCVD. Structural and optical characterizations have been carried out in order to (i) evaluate the Cd incorporation as a function of the growth parameters, (ii) measure the band gap evolution, (iii) assess the surface morphology, and (iv) determine the refractive index dispersion.

## II. EXPERIMENT

$\text{Zn}_{1-x}\text{Cd}_x\text{O}$  films were grown by MOCVD at relatively high temperatures, between 850 and 950 °C. Typically, the thickness was measured as about 300 nm. *R*-plane oriented sapphire substrates were used. These substrates were previously annealed at 1000 °C for 5 h under an oxygen atmosphere to reconstruct atomic steps and terraces on the surface. Diethyl zinc, dimethyl cadmium (DMCd), and nitrous oxide  $\text{N}_2\text{O}$  were chosen as the zinc, cadmium, and oxygen sources, respectively, and the carrier gas was helium. It has been previously reported that the use of high temperature processes with  $\text{N}_2\text{O}$  permits the growth of high quality ZnO epilayers.<sup>17</sup> Our horizontal MOCVD reactor, operating at 50 torr, allowed separate injection for group II (zinc and cadmium) and group VI (oxygen) precursors in order to avoid premature reactions in the manifold system. Growth parameters, such as substrate temperature, (DMCd/DEZn+DMCd) mole ratio in the gas phase, or VI/II mole ratio, were varied to investigate their influence on the Cd incorporation. Secondary ion mass spectrometry (SIMS, Cameca IMS3F) was used to characterize the depth profile of the cadmium composition. Aluminum concentrations were cal-

<sup>a)</sup>Electronic mail: sartel@cnrs-bellevue.fr

<sup>b)</sup>Author to whom correspondence should be addressed; electronic mail: sallet@cnrs-bellevue.fr

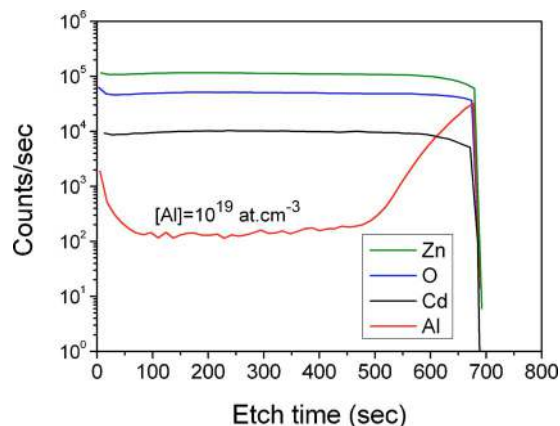


FIG. 1. (Color online) SIMS profile of a  $\text{Zn}_{0.945}\text{Cd}_{0.055}\text{O}$  layer grown at  $850^\circ\text{C}$ .

culated after measuring implanted standards. The surface morphology was assessed by scanning electron microscopy (SEM). PL measurements were carried out at 2 K, exciting the material with the deep uv lines (351 nm) of an argon ion laser. Ellipsometric measurements were carried out using a phase modulated spectroscopic ellipsometer (UVISSEL, Jobin-Yvon) at  $70^\circ$  incidence angle ( $70.69^\circ$  adjusted).

### III. RESULTS AND DISCUSSION

#### A. SIMS analysis

SIMS analysis first allowed us to check the incorporation of Cd atoms in the grown films. Figure 1 shows the typical depth profiles of the different elements detected in the samples, i.e., Zn, Cd, O, and Al. Flat Cd profiles were observed in all the layers, showing that the concentration is constant from the sapphire interface to the surface. Also, scanning ion images of the surface, filtered with Cd mass (not shown here), revealed a homogeneous planar distribution of the Cd atoms. This distribution suggests a random incorporation at the zinc sites, leading to a homogeneous  $\text{Zn}_{1-x}\text{Cd}_x\text{O}$  alloy. Moreover, x-ray diffraction measurements, not shown in this work, exhibit only one peak corresponding to (11 $\bar{2}$ 0) A-plane  $\text{ZnCdO}$ . No  $\text{CdO}$  cubic phase was observed. We also note from SIMS analysis a strong diffusion of the aluminum from the sapphire substrate, which is not surprising since high temperature processes were used. The Al diffusion may be prevented by depositing a thin  $\text{MgO}$  buffer layer at the interface. Farther away from the interface, the aluminum concentration within the layer is measured around  $10^{19}$  atoms  $\text{cm}^{-3}$ .

#### B. Photoluminescence and cadmium incorporation

Cd contents in the  $\text{Zn}_{1-x}\text{Cd}_x\text{O}$  films were indirectly evaluated after measuring the band gap shifts observed in PL experiments. According to our previous work<sup>15</sup> and report of Makino *et al.*,<sup>4</sup> we have considered, in first approximation, the following relationship between the alloy band gap shift and the Cd composition:

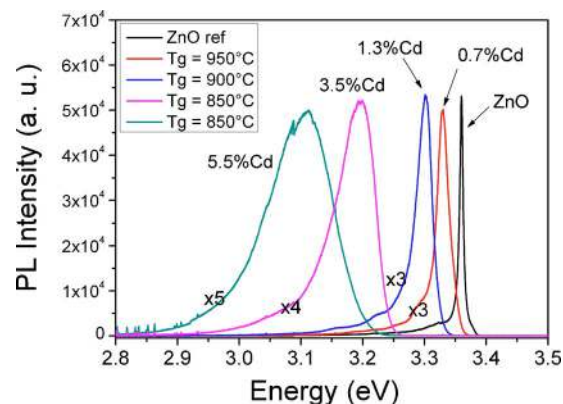


FIG. 2. (Color online) Low temperature (2 K) photoluminescence spectra of  $\text{Zn}_{1-x}\text{Cd}_x\text{O}$  films with various Cd concentrations, and pure ZnO reference sample.

$$\Delta E(\text{meV}) = 47x_{\text{Cd}}.$$

Figure 2 displays the low temperature photoluminescence spectra of four samples containing increasing Cd contents. A pure ZnO reference is given for comparison. We clearly see the band gap reduction due to  $\text{ZnO}$ - $\text{CdO}$  alloying up to 260 meV. The PL line shifts from a sharp near band edge emission at 3.36 eV in pure ZnO to a broadband centered at 3.1 eV. This value would correspond to an alloy containing 5.5% Cd. The observed broadening of the PL line with Cd concentration is mainly due to local fluctuation in the composition occurring at the atomic scale.<sup>18</sup> The lower growth temperature ( $850^\circ\text{C}$ ), used to grow layers with higher Cd contents, can also contribute to this broadening.

Figure 3(a) shows the Cd concentration as a function of the (DMCd/DEZn+DMCd) mole ratio in the gas phase. The growth temperature was  $850^\circ\text{C}$ . As expected, the efficiency of the cadmium incorporation is low. Increasing the DMCd concentration in the gas phase up to 50% linearly increases the incorporation of Cd in the solid solution up to 5.5%. A solubility limit is reached at this point. The use of Cd-rich conditions ( $R=0.66$ ) does not lead to further incorporation. The curve shows a plateau at around 5%.

In Fig. 3(b), the Cd concentration is plotted as a function of the growth temperature. It shows that Cd content decreases from 5.5% to 0.5% when  $T_g$  increases from 850 to  $950^\circ\text{C}$ . This result indicates a more effective incorporation of Cd atoms at lower temperatures. Growth temperatures above  $950^\circ\text{C}$  lead to a very weak Cd incorporation. Below  $850^\circ\text{C}$ , the crystalline quality becomes poor because the layers' diffraction intensity falls and surface morphology is very rough.

The mole ratio between group VI and group II precursors ( $R_{\text{VI/II}}$ ) ranged between 3100 and 7500, which is the typical range used for ZnO growth. The II-VI ratio has a strong effect on 2D growth. A low  $R_{\text{VI/II}}$ , in the range 100–1000, is used to grow ZnO nanowires, whereas a ratio above 3000 is needed to start to grow 2D films. In this work, no significant effect of  $R_{\text{VI/II}}$  was observed on the Cd composition of the  $\text{ZnCdO}$  layers.

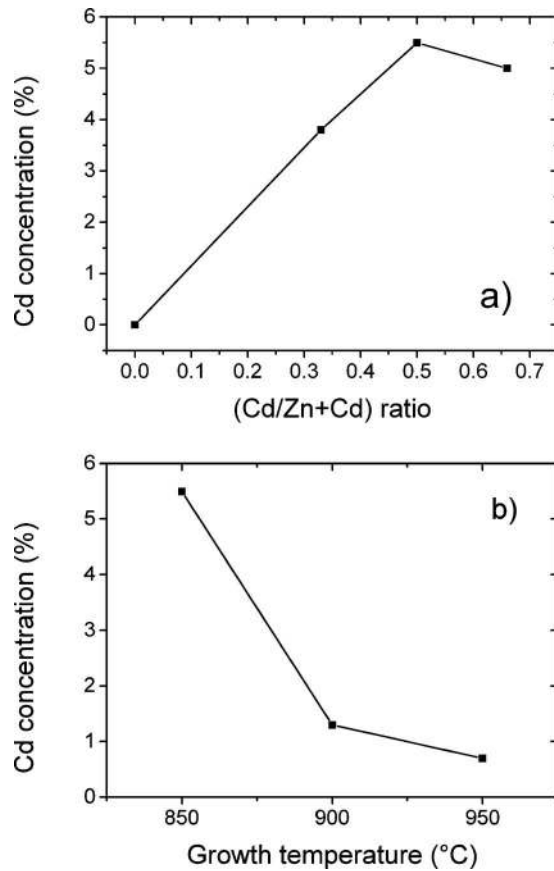


FIG. 3. Cadmium concentration of  $\text{Zn}_{1-x}\text{Cd}_x\text{O}$  films as a function of growth parameters: (a) varying the (Cd/Cd+Zn) ratio; (b) varying the growth temperature.

### C. Surface morphology

Figure 4 shows SEM images of two  $\text{Zn}_{1-x}\text{Cd}_x\text{O}$  films containing around 5% Cd. The surface morphology can be rather smooth. Some holelike defects with a triangular shape can be seen. This morphology is very similar to the one of pure ZnO film, indicating that the incorporation had no strong influence. Nevertheless, other samples exhibit rougher surfaces with elongated pyramidal defects oriented along the *C*-direction (not shown here). This nonuniformity from sample to sample could be attributed to the sapphire sub-

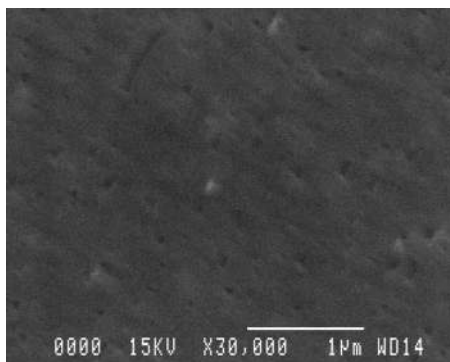


FIG. 4. SEM image of a  $\text{Zn}_{0.95}\text{Cd}_{0.05}\text{O}$  layer grown at 850 °C.

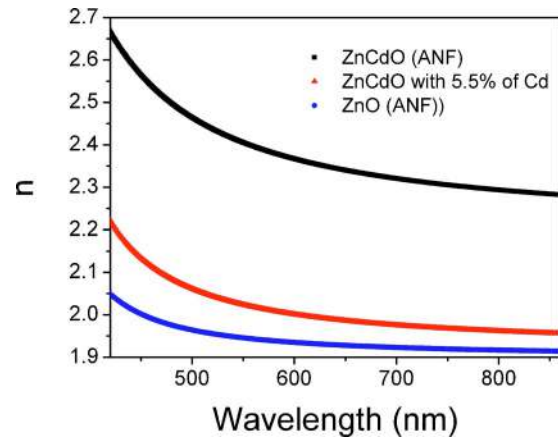


FIG. 5. (Color online) Refractive index dispersion of a 5.5% cadmium as retrieved from ellipsometric data. ZnO and ZnCdO dispersions using the Adachi–New Forouhi model are shown for comparison. The error bar on the retrieved data is about the thickness of the line.

strate preparation prior to growth. We have observed, using atomic force microscopy, that the surface reconstruction is sometimes not achieved over the whole 2" wafer, meaning some areas can be poorly reconstructed. As a consequence, layers grown on these areas exhibit rougher morphologies. This result could be inherent to our annealing furnace or due to nonuniformity in the wafer quality. We believe that this result could be the cause of the rough samples. This phenomenon is also observed in pure ZnO growth.

### D. Ellipsometry

Figure 5 shows the refractive index dispersion obtained from the 5.5% cadmium sample. The refractive index has been retrieved from ellipsometric data using the Sellmeier formula to account for the dispersion. Note that the analysis was limited to the below-band-gap range where absorption and scattering losses were supposed to be negligible. The Sellmeier parameters *A*, *B*, and  $\lambda_0$  were found to be 3.118, 0.592, and 345 nm, respectively. To model the virtual surface roughness, we used the effective medium approximation. The fitting parameters included two layer thicknesses (261 and 66 nm) and the void fraction (61%) for the top layer. The layer thicknesses including the top layer are in agreement with SEM observations. While the surface roughness of the film prevents a more detailed analysis, especially in the uv range where a more elaborate dispersion model than the Sellmeier model is needed, the retrieved refractive index lies in the expected range. Within the precision of the measurement (0.01), no optical anisotropy was observed. Refraction index dispersions of ZnO and ZnCdO using the Adachi–New Forouhi dispersion model<sup>19</sup> are shown for comparison. A more detailed comparison can be made using the results of Mares *et al.*<sup>16</sup> They obtained refractive indices at 600 nm of 1.99 and 2.03 for cadmium contents of 2% and 9%, respectively. We obtained a refractive index of 2 for a Cd content of about 5.5%. More detailed analysis like IR generalized ellipsometry, as demonstrated for *a*-plane ZnO,<sup>20</sup> will follow the sample interface quality improvement.

#### IV. SUMMARY AND CONCLUSIONS

In summary, the growth of  $\text{Zn}_{1-x}\text{Cd}_x\text{O}$  alloys by MOCVD technique has been successful up to 5.5% Cd. SIMS analysis showed that homogeneous composition within the sample depth and rather smooth morphologies can be obtained. The Cd composition is found to be strongly dependant on the growth temperature. At 5.5% Cd incorporation, the photoluminescence emission at 2 K shows a redshift of 260 meV. Ellipsometric measurements reveal an increase of the refractive index from 1.94 to 2 at 600 nm.

#### ACKNOWLEDGMENT

This work was supported by French Agence Nationale de la Recherche (ANR) in the framework of the ULTRAFLU project.

<sup>1</sup>A. Ohtomo, M. Kawasaki, T. Koida, K. Masubuchi, H. Koinuma, Y. Sakurai, Y. Yoshida, T. Yasuda, and Y. Segawa, *Appl. Phys. Lett.* **72**, 2466 (1998).

<sup>2</sup>W. I. Park, Gyu-Chul Yi, and H. M. Jang, *Appl. Phys. Lett.* **79**, 2022 (2001).

<sup>3</sup>Y. R. Ryu, T. S. Lee, J. A. Lubguban, A. B. Corman, H. W. White, J. H. Leem, M. S. Han, Y. S. Park, C. J. Youn, and W. J. Kim, *Appl. Phys. Lett.* **88**, 052103 (2006).

<sup>4</sup>T. Makino, Y. Segawa, M. Kawasaki, A. Ohtomo, R. Shiroki, K. Tamura, T. Yasuda, and H. Koinuma, *Appl. Phys. Lett.* **78**, 1237 (2001).

<sup>5</sup>K. Sakurai, T. Kubo, D. Kajita, T. Tanabe, H. Takasu, Shizuo Fujita, and Shigeo Fujita, *Jpn. J. Appl. Phys., Part 2* **39**, L1146 (2000).

<sup>6</sup>Th. Gruber, C. Kirchner, R. Kling, F. Reuss, A. Waag, F. Bertram, D. Forster, J. Christen, and M. Schreck, *Appl. Phys. Lett.* **83**, 3290 (2003).

<sup>7</sup>C. Morhain, X. Tang, M. Teisseire Doninelli, B. Lo, J. M. Chauveau, B. Vinter, O. Tottereau, P. Vennéguès, C. Deparis, and G. Neu, *Superlattices Microstruct.* **38**, 455 (2005).

<sup>8</sup>A. Tsukazaki, A. Ohtomo, T. Kita, Y. Ohno, H. Ohno, and M. Kawasaki, *Science* **315**, 1388 (2007).

<sup>9</sup>S. Sadofev, S. Blumstengel, J. Cui, J. Puls, S. Rogaschewski, P. Schäfer, and F. Henneberger, *Appl. Phys. Lett.* **89**, 201907 (2006).

<sup>10</sup>S. Shigemori, A. Nakamura, J. Ishihara, T. Aoki, and J. Temmyo, *Jpn. J. Appl. Phys., Part 2* **43**, L1088 (2004).

<sup>11</sup>J. Zúñiga-Pérez, V. Muñoz-Sanjose, M. Lorenz, G. Benndorf, S. Heitsch, D. Spemann, and M. Grundmann, *J. Appl. Phys.* **99**, 023514 (2006).

<sup>12</sup>C. W. Sun, P. Xin, C. Y. Ma, Z. W. Liu, Q. Y. Zhang, Y. Q. Wang, Z. J. Yin, S. Huang, and T. Chen, *Appl. Phys. Lett.* **89**, 181923 (2006).

<sup>13</sup>A. Mohanta and R. K. Thareja, *J. Appl. Phys.* **103**, 024901 (2008).

<sup>14</sup>J. Ishihara, A. Nakamura, S. Shigemori, T. Aoki, and J. Temmyo, *Appl. Phys. Lett.* **89**, 091914 (2006).

<sup>15</sup>A. Lusson, N. Haneche, V. Sallet, P. Galtier, V. Munoz-Sanjose, J. Zuniga-Perez, S. Agouram, and J. Bastos Segura, *J. Korean Phys. Soc.* **53**, 158 (2008).

<sup>16</sup>J. W. Mares, M. Falanga, W. R. Folks, G. Boreman, A. Osinsky, B. Hertog, J. Q. Xie, and W. V. Schoenfeld, *J. Electron. Mater.* **37**, 1665 (2008).

<sup>17</sup>S. Heinze, A. Krtischil, J. Blasing, T. Hempel, P. Veit, A. Dadgar, J. Christen, and A. Krost, *J. Cryst. Growth* **308**, 170 (2007).

<sup>18</sup>A. Lusson, R. Legros, Y. Marfaing, and H. Mariette, *Solid State Commun.* **67**, 851 (1988).

<sup>19</sup>H. Yoshikawa and S. Adachi, *Jpn. J. Appl. Phys., Part 1* **36**, 6237 (1997).

<sup>20</sup>C. Bundesmann, N. Ashkenov, M. Schubert, A. Rahm, H. v. Wenckstern, E. M. Kaidashev, M. Lorenz, and M. Grundmann, *Thin Solid Films* **455–456**, 161 (2004).